Environmental Science & Technology Letters

Letter

pubs.acs.org/journal/estlcu

A pH-Gradient Flow Cell for Converting Waste CO_2 into Electricity

Taeyoung Kim, Bruce E. Logan, and Christopher A. Gorski*

Department of Civil and Environmental Engineering, The Pennsylvania State University, University Park, Pennsylvania 16802, United States

Supporting Information

ABSTRACT: The CO_2 concentration difference between ambient air and exhaust gases created by combusting fossil fuels is an untapped energy source for producing electricity. One method of capturing this energy is dissolving CO_2 gas into water and then converting the produced chemical potential energy into electrical power using an electrochemical system. Previous efforts using this method found that electricity can be generated; however, electrical power densities were low, and expensive ion-exchange membranes were needed. Here, we overcame these challenges by developing a new approach to capture electrical power from CO_2 dissolved in water, the pH-gradient flow cell. In this approach, two identical supercapacitive manganese oxide electrodes were separated by a nonselective membrane and exposed to an aqueous buffer solution sparged with either CO_2 gas or air. This pH-gradient flow cell produced an average power density of 0.82 W/m^2, which was nearly 200 times higher than values reported using previous approaches.

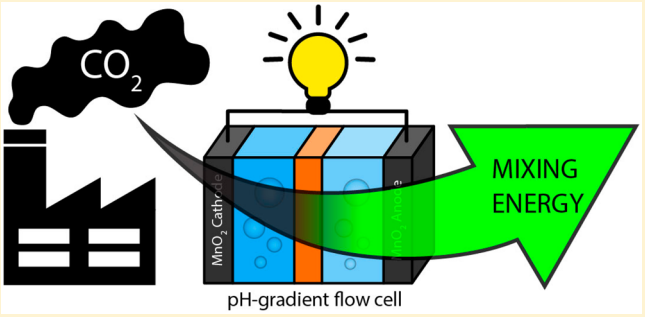

pH-gradient flow cell

INTRODUCTION

Carbon dioxide (CO_2) is produced and released into the atmosphere when fossil fuels are combusted, contributing to global climate change. While there is a clear long-term need to make the transition to energy-producing technologies that do not generate CO_2, there is also a critical short-term need to reduce overall CO_2 emissions by harvesting the potential energy contained in CO_2 exhaust. Previous work has estimated that the theoretical total amount of potential energy that is produced from CO_2 emissions annually is approximately 1570 TWh,[1] which is more than one-third of the total U.S. electricity generated in 2015 (4078 TWh).[2] The most extensively studied approach for capturing this energy is to use catalytic processes to convert emitted CO_2 into a fuel, such as hydrocarbons and syngas, which can subsequently be fed into a fuel cell along with other energy dense fuels, such as H_2, to generate electrical power.[3,4] Here, we examine an alternative strategy that has been investigated to a lesser degree, which is based on recently developed approaches to produce electrical power from differences in salt concentrations between two waters using electrochemical cells (e.g., refs 5−15). In the study presented here, we used the CO_2 concentration difference between exhaust gas and atmospheric air[16] to create pH differences between two waters, which could subsequently be used to generate electricity.[1,17,18]

When CO_2 is dissolved in water, it forms carbonic acid (H_2CO_3), which disproportionates into bicarbonate (HCO_3^-) and protons (H^+) at neutral and basic pHs. Prior work has shown that flowing solutions containing dissolved CO_2 and industrial alkaline wastes through different compartments in a fuel cell divided by ion-exchange membranes can be used to generate a voltage across the membranes while mineralizing CO_2.[17] This approach yielded a power density of 5.5 W/m^2 but required chemical inputs [i.e., N_2, H_2, and $Ca(OH)_2$] that would make the process difficult to implement universally. Carbon dioxide can also be used to generate electrical power without the need for additional resources by creating differences in pH values or bicarbonate concentrations between two solutions. Recently, this approach was shown to produce electricity from CO_2- and air-sparged solutions using solid film and flow capacitive electrodes.[1,18] While this approach produced electricity, there were two practical challenges that would limit its practical use. First, reported power densities were low (0.0045 W/m^2).[1,18] Second, these systems required ion-exchange membranes that would be prohibitively expensive relative to the achievable power densities.[1,17−19] Therefore, new technological advances are necessary to increase power densities and reduce material costs to make the proposed approach economically viable.

Here we developed and tested a novel electrochemical pH-gradient flow cell for producing electricity from the pH difference generated from CO_2- and air-sparged aqueous solutions. We hypothesized that manganese oxide (MnO_2) electrodes could be used to rapidly develop pH-dependent electrode potentials and hence produce electricity (Figure 1a). While MnO_2 has been extensively studied in the past because of its use as a catalyst, a supercapacitor in energy storage devices, and an electrode material in salinity-gradient energy technologies,[9,20−23] no work

Received: December 13, 2016
Revised: January 9, 2017
Accepted: January 12, 2017
Published: January 12, 2017

DOI: 10.1021/acs.estlett.6b00467
Environ. Sci. Technol. Lett. 2017, 4, 49−53

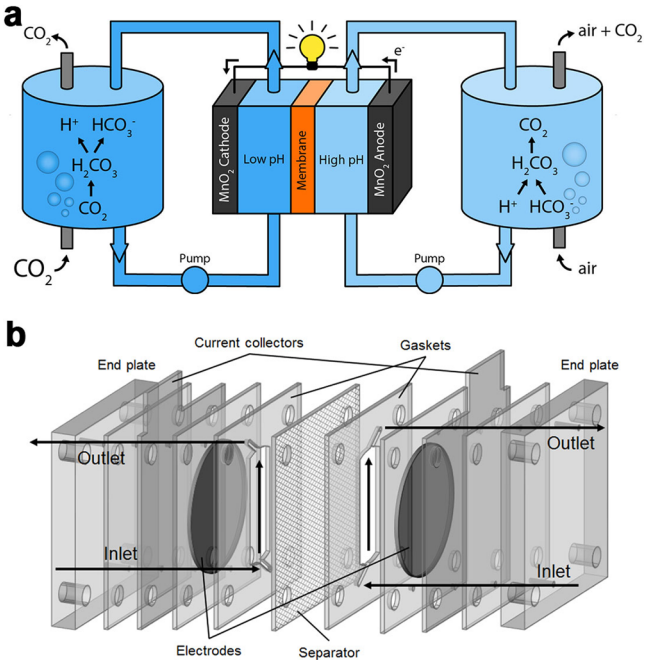

Figure 1. (a) Schematic of the pH-gradient flow cell for converting CO_2 into electricity. The flow cell consisted of two identical MnO_2 electrodes (black) divided by a nonselective membrane (orange) placed between channels. The channels were simultaneously fed 1 M $NaHCO_3$ solutions with a lower pH value (7.7, dark blue) or a higher pH value (9.4, light blue) that was generated by sparging the solutions with CO_2 (pH 7.7) or air (pH 9.4), respectively. (b) Detailed diagram illustrating the components of the flow cell.

has previously investigated if MnO_2 electrodes could be used to generate electricity from pH-dependent electrode potentials. In the flow cell, the MnO_2 electrodes were separated by an inexpensive, nonselective membrane and were each exposed to two different aqueous solutions containing sodium bicarbonate buffer: one sparged with CO_2 gas, and the other sparged with air. Here we demonstrated the feasibility of this approach by showing power production as a function of external resistance over multiple cycles, compared to the measured cell voltage with the predicted value from the Nernst equation, and outlined how this cell could be improved for increased power production.

MATERIALS AND METHODS

MnO_2 was synthesized by following a previously reported coprecipitation method.[24,25] Briefly, a 0.2 M $MnSO_4$ solution (120 mL, Alfa Aesar) was poured into a 0.2 M $KMnO_4$ solution (80 mL, Alfa Aesar) while it was being vigorously stirred at room temperature. The resulting MnO_2 precipitates were washed and collected by centrifugation, followed by overnight drying in a vacuum oven at 70 °C. To prepare composite electrodes, MnO_2 powder (70 wt %), carbon black (20 wt %, Vulcan XC72R, Cabot), and polyvinylidenefluoride (10 wt %, kynar HSV 900, Arkema Inc.) were mixed homogeneously in 1-methyl-2-pyrrolidinone (2 mL per 0.1 g of MnO_2, Sigma-Aldrich). The resulting slurry was loaded dropwise onto carbon cloth (1071HCB, AvCarb Material Solutions), where the mass loading of the composite electrode was approximately 4–5 mg/cm^2, which was chosen as an optimal condition for power production (data not shown). Afterward, the electrodes were dried overnight in a vacuum oven at 70 °C. Additional details regarding the characterizations of the MnO_2, flow cell construction, and the electrode potential of MnO_2 as a function of pH are provided in sections A and B of the Supporting Information.

To convert the CO_2 concentration difference between exhaust gas and ambient air into electricity using MnO_2 electrodes in a flow cell, two 1 M $NaHCO_3$ solutions were sparged using a gas diffuser stone and stirred using either pure CO_2 (final pH of 7.7) or air (final pH of 9.4) to produce a pH difference between the solutions (ΔpH = 1.7). Each solution was simultaneously injected into one of the two channels in the flow cell using a peristaltic pump (Cole-Parmer) at a flow rate of 15 mL/min that was large enough to maintain the pH difference between two channels and hence to develop the pseudoequilibrium cell voltage.[26] Electricity produced by connecting two electrodes was measured at different external resistances (R_{ext} = 4, 6, 10, 16, and 22 Ω). During electricity production, the cell voltage (ΔE_{cell}) was recorded using a potentiostat (VMP3, Bio-Logic). A cycle was completed when the cell voltage decreased below ±30 mV, and a new cycle was initiated by switching the solutions to the alternate channels.

The power density of a cycle was calculated using the cell voltage and the external resistance ($P = \Delta E_{cell}^2/R_{ext}$) divided by the membrane area (~3 cm^2). The average power density (P_{avg}) was calculated over the complete cycle, which produced the energy density (W) when multiplied by time. Note that a conventional method (i.e., constant current discharging) can also be used to produce electricity, but the power density calculated using this method would account for only the discharging process. The method for recording the cell voltage while connecting the external resistance during the entire process provides a power density that includes the time taken for switching solutions and developing the cell voltage (i.e., the charging process).

RESULTS AND DISCUSSION

In this flow cell system, we created a pH gradient between two aqueous solutions by sparging 1 M $NaHCO_3$ with either air (pH 9.4) or CO_2 (pH 7.7). These two solutions were then pumped through the two channels in the flow cell, and each contained an identical electrode composed of amorphous MnO_2 (Figure 1b). The difference in pH between the two solutions created a voltage difference between the two electrodes of 0.196 ± 0.001 V (Figure 2a) when the circuit was open. Periodically alternating which solution flowed through each channel yielded a reversal in the cell voltage that developed within 60 s.

To examine the relationship between the solution pH and the MnO_2 electrode potential, we measured open-circuit potentials of a MnO_2 electrode in several sodium bicarbonate/carbonate solutions with pH values ranging from 7.7 and 11.9 and a constant Na^+ concentration of 1 M. The MnO_2 electrode potential decreased as the solution pH increased, with the potential being linearly proportional to the pH with a slope of −0.059 V/pH unit (Figure 2b). Previous work has found that structural Mn^{3+} and Mn^{4+} in MnO_2 can undergo a reversible redox reaction through the intercalation/deintercalation and/or adsorption/desorption of protons or cations (i.e., Na^+ in this system) according to the following half-reactions:[21,27−30]

$$MnO_{2(s)} + H^+ + e^- = MnOOH_{(s)} \quad (1)$$

$$MnO_{2(s)} + Na^+ + e^- = MnOONa_{(s)} \quad (2)$$

In our system, the Na^+ concentrations (and activities) were the same in all the solutions, and therefore, the relative potential

DOI: 10.1021/acs.estlett.6b00467
Environ. Sci. Technol. Lett. 2017, 4, 49−53

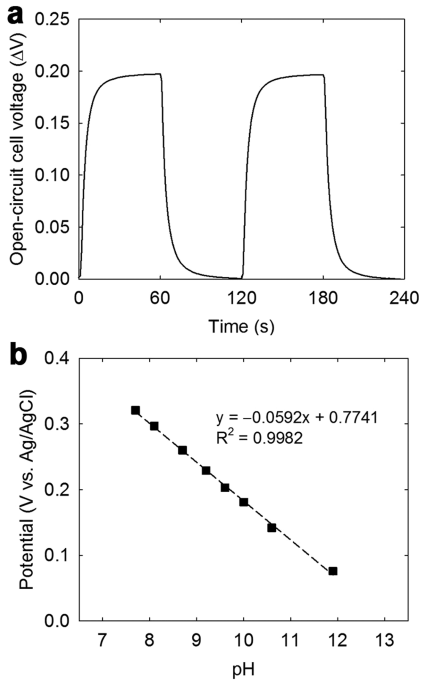

Figure 2. (a) Open-circuit cell voltage profile of a full cell measured by switching the injection of CO_2- and air-sparged 1 M $NaHCO_3$ solutions (ΔpH = 1.7) every 60 s at a flow rate of 15 mL/min. (b) Open-circuit potential of the MnO_2 electrode as a function of pH measured in a half-cell consisting of a platinum counter electrode and a Ag/AgCl reference electrode. Solutions at pH 7.7−11.9 was prepared by mixing 1 M $NaHCO_3$ and 0.5 M Na_2CO_3 solutions in different ratios.

difference between the electrodes was due to the pH difference according to eq 1. The Nernst equation for eq 1 can be written as

$$E = E^0 + \frac{RT}{F} \ln a_{H^+} \quad (3)$$

where E is the electrode potential, E^0 is the standard electrode potential, R is the gas constant (8.314 J mol^{-1} K^{-1}), T is absolute temperature (kelvin), F is the Faraday constant (96485 C mol^{-1}), a is activity, and the activity of each solid is assumed to be 1. At room temperature (25 °C), the Nernst equation can be rewritten as

$$E = E^0 - 0.059 \times \text{pH} \quad (4)$$

The predicted pH dependency from eq 4 (−0.059 V/pH unit) was in excellent agreement with experimental data shown in Figure 2b (−0.059 V/pH unit). In addition, the theoretical estimation made by applying the pH difference between CO_2- and air-sparged solutions (ΔpH = 1.7) shown in Figure 2a to eq 4 (0.201 V) also resulted in good agreement with the cell voltage achieved in the flow cell (0.196 V).

To convert the cell voltage that was developed in the flow cell into electricity, the circuit was closed using an external resistor (R_{ext} = 22 Ω) while passing the CO_2-sparged and air-sparged solutions through each channel. When the circuit was closed, the cell voltage rapidly increased over the first 5 s and then gradually decreased as the cell discharged (Figure 3a). The reason that the voltage initially increased and then decreased was that two competing factors were affecting it: (1) the cell voltage increased because the MnO_2 electrodes were developing pH-dependent potentials upon being exposed to the solutions (eqs 3 and 4), resulting in charging of the cell, and (2) electrical power was

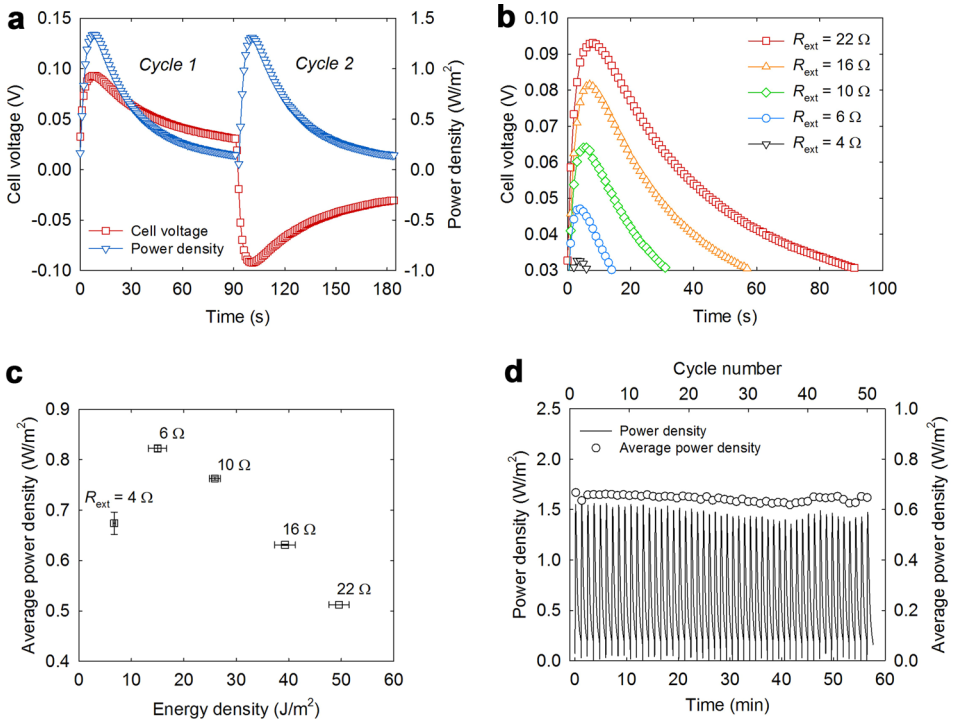

Figure 3. (a) Representative cell voltage and power density profiles for the pH-gradient flow cell (R_{ext} = 22 Ω). A cycle (cycle 1) started by switching the flow path between CO_2- and air-sparged 1 M $NaHCO_3$ solutions and ended when the cell voltage decreased below ±30 mV. Switching the flow path produced power in the sequel cycle (cycle 2) and reversed the cell voltage. (b) Representative cell voltage profiles. (c) Average power density vs energy density plot as a function of load placed between electrodes. The error bars denote the range for duplicated experiments. (d) Long-term cycle performance for 50 cycles (R_{ext} = 16 Ω).

DOI: 10.1021/acs.estlett.6b00467
Environ. Sci. Technol. Lett. 2017, 4, 49−53

being produced as a result of the potential difference between the electrodes (i.e., the cell voltage), which decreased the cell voltage as a result of discharging of the cell through redox reactions (eqs 1 and 2). On the basis of the cell voltage and current flow, we calculated an average power density of 0.52 W/m^2 of membrane area. After the first discharge, additional electricity could be produced by switching the solutions that flowed over each electrode, resulting in a similar average power density of 0.51 W/m^2 in the opposite direction. Switching the flow path between the low- and high-pH solutions altered the electrode potentials and reversed the cell charging/discharging mechanism, allowing the discharged electrodes to recharge.

To optimize the power production of the pH-gradient flow cell, we measured cell voltage profiles as a function of external resistance. Decreasing the external resistance from 22 to 4 Ω led to an increase in current flow between the electrodes and a decrease in cell voltage, due to an increase in the ohmic drop (Figure 3b). For each resistance, we calculated the energy and average power densities. We achieved the highest average power density (0.82 ± 0.01 W/m^2) and energy density (15.00 ± 1.74 J/m^2) when R_{ext} was 6 Ω (Figure 3c). Note that the average power density increased to 1.70 W/m^2 using the highest achievable pH difference between pure CO_2 and ambient air [i.e., pH_1 = 7.6, and pH_2 = 10.0 (see section D of the Supporting Information)]. To examine the power production of the flow cell over prolonged periods, we tested the performance over 50 cycles at an R_{ext} of 16 Ω by periodically alternating the solutions that flowed into each channel. We observed stable average power densities for 50 cycles (Figure 3d), indicating that the electrodes underwent reversible reactions. The average power density was approximately 0.66 ± 0.01 W/m^2 for the first 10 cycles, which decreased to 0.64 ± 0.01 W/m^2 for the last 10 cycles (2% decrease).

To produce the high average power and energy densities demonstrated here, the cell design and solution chemistry played important roles. The MnO_2 electrodes developed pH-dependent potentials that could be constantly discharged; thus, electricity was continually produced without the need for an additional step for charging using a secondary device (e.g., a potentiostat). The use of $NaHCO_3$ solutions also enhanced electricity production in multiple ways. First, it kept the pH above 7, which was important because the MnO_2 electrodes could become destabilized in acidic solutions.[31] Second, the ability of bicarbonate to buffer the pH provided a source of protons at the electrode surface, which yielded an achievable charge storage capacity that was more than double what was achieved using NaCl as an electrolyte (Figure S5). Third, the use of $NaHCO_3$ solutions allowed for the rapid cell voltage development for the faradaic reaction. The quick equilibration time was due in part to the pH buffering of the bicarbonate in solution. In a control experiment conducted with 1 M NaCl solutions (ΔpH = 1.7), the voltage difference reached only approximately 0.08 V after 250 s (Figure S6), suggesting that the bicarbonate ions served as proton donors and/or acceptors near the electrode surface. Fourth, the $NaHCO_3$ solutions did not require additional inputs other than CO_2 gas and can likely be combined with nonprecious salt solutions such as brackish water.

In this report, high power densities were achieved when converting waste CO_2 into electricity using the pH difference between CO_2- and air-sparged solutions with a pH-gradient flow cell. By using MnO_2 electrodes that developed pH-dependent potentials, we were able to produce an average power density (0.82 W/m_2) that was nearly 200 times higher than what has previously been reported.[1,18] This power density was comparable to those produced in salinity-gradient technologies (0.1−10 W/m^2) that use similar cell designs to produce electricity from seawater and river water.[9,32−34] The power densities were relatively low, however, compared to those of other fuel cell systems that use CO_2 (1−10 kW/m^2).[3,4] There are two reasons for this. (1) The fuel cell systems require other energy dense fuels, such as H_2, and elevated temperatures, which increase the amount of potential energy available, and (2) fuel cell technologies have been studied far more extensively than the technology discussed here and therefore are further along in their development and optimization. The cell described here has advantages over these technologies in that it uses only inexpensive materials and can be operated at room temperature. In addition, operating our system was focused on maximizing the power density; thus, the amount of energy harvested would be only a portion of the available energy between two solutions because of the inherent trade-off between the maximal power and energy recovery efficiency.[5] Our calculations indicated that the amount of harvestable energy normalized to the volume of a mixed solution (0.295 kJ/L) or the mass of CO_2 (76.8 kJ/kg) was more than twice as large as the energy inputs needed for sparging and pumping (see section E of the Supporting Information). Note, however, that the relative values would certainly change when scaling up the technology for real-world applications due to variations in the flue gas physical properties and chemistry, specifically the CO_2 concentration (typical values are approximately 10%, but they can vary depending on the source),[35] the flue gas temperature after cooling (40−60 °C),[36] and the impurities present in the gas stream (e.g., sulfur). Additional energy would also be consumed for separating CO_2 from a flue gas and constructing reactor components. We note, however, that determining if this process would be economically viable when scaled up would require a full energy return on investment. At this stage, the results demonstrated here indicate that the pH-gradient flow could represent a promising approach for converting CO_2 into electricity, but further investigations aimed at optimizing performance and assessing energy balance are needed.

■ ASSOCIATED CONTENT

Supporting Information

The Supporting Information is available free of charge on the ACS Publications website at DOI: 10.1021/acs.estlett.6b00467.

Detailed information about the electrode material characterizations, reactor construction, electrochemical characterizations, and energy calculations (PDF)

■ AUTHOR INFORMATION

Corresponding Author

*E-mail: gorski@engr.psu.edu. Phone: +1-814-865-5673. Fax: +1-814-863-7304.

ORCID

Bruce E. Logan: 0000-0001-7478-8070

Christopher A. Gorski: 0000-0002-5363-2904

Notes

The authors declare no competing financial interest.

■ ACKNOWLEDGMENTS

This research was supported by the National Science Foundation through Grants CBET-1464891 and CBET-1603635 and internal seed grant funding from the Penn State Institutes for

DOI: 10.1021/acs.estlett.6b00467
Environ. Sci. Technol. Lett. 2017, 4, 49−53

Energy and the Environment (PSIEE) and the Materials Research Institute (MRI).

REFERENCES

(1) Hamelers, H.; Schaetzle, O.; Paz-García, J.; Biesheuvel, P.; Buisman, C. Harvesting energy from CO_2 emissions. *Environ. Sci. Technol. Lett.* **2014**, *1* (1), 31−35.

(2) Electric Power Annual 2014. http://www.eia.gov/electricity/annual/html/epa_01_01.html (accessed December 12, 2016).

(3) Steele, B. C. H.; Heinzel, A. Materials for fuel-cell technologies. *Nature* **2001**, *414* (6861), 345−352.

(4) Kondratenko, E. V.; Mul, G.; Baltrusaitis, J.; Larrazábal, G. O.; Pérez-Ramírez, J. Status and perspectives of CO_2 conversion into fuels and chemicals by catalytic, photocatalytic and electrocatalytic processes. *Energy Environ. Sci.* **2013**, *6* (11), 3112−3135.

(5) Yip, N. Y.; Brogioli, D.; Hamelers, H. V.; Nijmeijer, K. Salinity Gradients for Sustainable Energy: Primer, Progress, and Prospects. *Environ. Sci. Technol.* **2016**, *50* (22), 12072−12094.

(6) Hatzell, M. C.; Hatzell, K. B.; Logan, B. E. Using flow electrodes in multiple reactors in series for continuous energy generation from capacitive mixing. *Environ. Sci. Technol. Lett.* **2014**, *1* (12), 474−478.

(7) Hatzell, M. C.; Raju, M.; Watson, V. J.; Stack, A. G.; van Duin, A. C.; Logan, B. E. Effect of strong acid functional groups on electrode rise potential in capacitive mixing by double layer expansion. *Environ. Sci. Technol.* **2014**, *48* (23), 14041−14048.

(8) Kim, T.; Rahimi, M.; Logan, B. E.; Gorski, C. A. Harvesting Energy from Salinity Differences Using Battery Electrodes in a Concentration Flow Cell. *Environ. Sci. Technol.* **2016**, *50* (17), 9791−9797.

(9) La Mantia, F.; Pasta, M.; Deshazer, H. D.; Logan, B. E.; Cui, Y. Batteries for efficient energy extraction from a water salinity difference. *Nano Lett.* **2011**, *11* (4), 1810−1813.

(10) Sales, B.; Saakes, M.; Post, J.; Buisman, C.; Biesheuvel, P.; Hamelers, H. Direct power production from a water salinity difference in a membrane-modified supercapacitor flow cell. *Environ. Sci. Technol.* **2010**, *44* (14), 5661−5665.

(11) Vermaas, D. A.; Bajracharya, S.; Sales, B. B.; Saakes, M.; Hamelers, B.; Nijmeijer, K. Clean energy generation using capacitive electrodes in reverse electrodialysis. *Energy Environ. Sci.* **2013**, *6* (2), 643−651.

(12) Logan, B. E.; Elimelech, M. Membrane-based processes for sustainable power generation using water. *Nature* **2012**, *488* (7411), 313−319.

(13) Moreno, J.; Slouwerhof, E.; Vermaas, D.; Saakes, M.; Nijmeijer, K. The Breathing Cell: Cyclic Intermembrane Distance Variation in Reverse Electrodialysis. *Environ. Sci. Technol.* **2016**, *50* (20), 11386−11393.

(14) Post, J. W.; Hamelers, H. V.; Buisman, C. J. Energy recovery from controlled mixing salt and fresh water with a reverse electrodialysis system. *Environ. Sci. Technol.* **2008**, *42* (15), 5785−5790.

(15) Długołęcki, P.; van der Wal, A. Energy recovery in membrane capacitive deionization. *Environ. Sci. Technol.* **2013**, *47* (9), 4904−4910.

(16) Gellender, M. A proposed new energy source: The "mixing energy" of engine exhaust gas. *J. Renewable Sustainable Energy* **2010**, *2* (2), 023101.

(17) Xie, H.; Wang, Y.; He, Y.; Gou, M.; Liu, T.; Wang, J.; Tang, L.; Jiang, W.; Zhang, R.; Xie, L.; Liang, B. Generation of electricity from CO_2 mineralization: Principle and realization. *Sci. China: Technol. Sci.* **2014**, *57* (12), 2335−2343.

(18) Porada, S.; Weingarth, D.; Hamelers, H. V.; Bryjak, M.; Presser, V.; Biesheuvel, P. Carbon flow electrodes for continuous operation of capacitive deionization and capacitive mixing energy generation. *J. Mater. Chem. A* **2014**, *2* (24), 9313−9321.

(19) Ramon, G. Z.; Feinberg, B. J.; Hoek, E. M. Membrane-based production of salinity-gradient power. *Energy Environ. Sci.* **2011**, *4* (11), 4423−4434.

(20) Zhang, Z.; Liu, J.; Gu, J.; Su, L.; Cheng, L. An overview of metal oxide materials as electrocatalysts and supports for polymer electrolyte fuel cells. *Energy Environ. Sci.* **2014**, *7* (8), 2535−2558.

(21) Augustyn, V.; Simon, P.; Dunn, B. Pseudocapacitive oxide materials for high-rate electrochemical energy storage. *Energy Environ. Sci.* **2014**, *7* (5), 1597−1614.

(22) Ma, Z.; Yuan, X.; Li, L.; Ma, Z.-F.; Wilkinson, D. P.; Zhang, L.; Zhang, J. A review of cathode materials and structures for rechargeable lithium-air batteries. *Energy Environ. Sci.* **2015**, *8* (8), 2144−2198.

(23) Ye, M.; Pasta, M.; Xie, X.; Cui, Y.; Criddle, C. S. Performance of a mixing entropy battery alternately flushed with wastewater effluent and seawater for recovery of salinity-gradient energy. *Energy Environ. Sci.* **2014**, *7* (7), 2295−2300.

(24) Brousse, T.; Toupin, M.; Dugas, R.; Athouël, L.; Crosnier, O.; Bélanger, D. Crystalline MnO_2 as possible alternatives to amorphous compounds in electrochemical supercapacitors. *J. Electrochem. Soc.* **2006**, *153* (12), A2171−A2180.

(25) Toupin, M.; Brousse, T.; Bélanger, D. Influence of microstucture on the charge storage properties of chemically synthesized manganese dioxide. *Chem. Mater.* **2002**, *14* (9), 3946−3952.

(26) Długołęcki, P.; Gambier, A.; Nijmeijer, K.; Wessling, M. Practical Potential of Reverse Electrodialysis As Process for Sustainable Energy Generation. *Environ. Sci. Technol.* **2009**, *43* (17), 6888−6894.

(27) Toupin, M.; Brousse, T.; Bélanger, D. Charge storage mechanism of MnO_2 electrode used in aqueous electrochemical capacitor. *Chem. Mater.* **2004**, *16* (16), 3184−3190.

(28) Vinny, R. T.; Chaitra, K.; Venkatesh, K.; Nagaraju, N.; Kathyayini, N. An excellent cycle performance of asymmetric supercapacitor based on bristles like α-MnO2 nanoparticles grown on multiwalled carbon nanotubes. *J. Power Sources* **2016**, *309*, 212−220.

(29) Yu, Z.; Duong, B.; Abbitt, D.; Thomas, J. Highly ordered MnO_2 nanopillars for enhanced supercapacitor performance. *Adv. Mater.* **2013**, *25* (24), 3302−3306.

(30) Lee, H. Y.; Goodenough, J. B. Supercapacitor behavior with KCl electrolyte. *J. Solid State Chem.* **1999**, *144* (1), 220−223.

(31) Long, J. W.; Rhodes, C. P.; Young, A. L.; Rolison, D. R. Ultrathin, protective coatings of poly (o-phenylenediamine) as electrochemical proton gates: making mesoporous MnO_2 nanoarchitectures stable in acid electrolytes. *Nano Lett.* **2003**, *3* (8), 1155−1161.

(32) Yip, N. Y.; Tiraferri, A.; Phillip, W. A.; Schiffman, J. D.; Hoover, L. A.; Kim, Y. C.; Elimelech, M. Thin-Film Composite Pressure Retarded Osmosis Membranes for Sustainable Power Generation from Salinity Gradients. *Environ. Sci. Technol.* **2011**, *45* (10), 4360−4369.

(33) Liu, F.; Schaetzle, O.; Sales, B. B.; Saakes, M.; Buisman, C. J.; Hamelers, H. V. Effect of additional charging and current density on the performance of Capacitive energy extraction based on Donnan Potential. *Energy Environ. Sci.* **2012**, *5* (9), 8642−8650.

(34) Vermaas, D. A.; Saakes, M.; Nijmeijer, K. Doubled power density from salinity gradients at reduced intermembrane distance. *Environ. Sci. Technol.* **2011**, *45* (16), 7089−7095.

(35) Rao, A. B.; Rubin, E. S. A technical, economic, and environmental assessment of amine-based CO_2 capture technology for power plant greenhouse gas control. *Environ. Sci. Technol.* **2002**, *36* (20), 4467−4475.

(36) Espinal, L.; Poster, D. L.; Wong-Ng, W.; Allen, A. J.; Green, M. L. Measurement, Standards, and Data Needs for CO_2 Capture Materials: A Critical Review. *Environ. Sci. Technol.* **2013**, *47* (21), 11960−11975.

DOI: 10.1021/acs.estlett.6b00467
Environ. Sci. Technol. Lett. 2017, 4, 49−53